Supporting Information

Two novel bi-functional hybrid materials constructed from POMs and Schiff base with excellent third-order NLO and catalytic properties

Gonghao Hu[a], Hao Miao[a], Hua Mei,*[a] Shuai Zhou[a] and Yan Xu*[a, b]

[a]College of Chemistry and Chemical Engineering, State Key Laboratory of Materials-Oriented Chemical Engineering, Nanjing Tech University, Nanjing 210009, P. R. China

[b]Coordination Chemistry Institute, State Key Laboratory of Coordination Chemistry, Nanjing University, Nanjing 210093, P. R. China

1. Materials and Methods

2, 6-diacetylpyridine bis-(semicarbazone) (DAPSC) and potassium borotungstate ($K_5BW_{12}O_{40}$) were prepared according to the literature. Other chemicals were purchased from commercial sources and used without further purification. Element analyses for C, H, and N were implemented on a Perkin-Elmer 2400 CHN elemental analyzer. IR spectra were recorded on KBr pellets with a Nicolet Impact 410 FTIR spectrometer in the range of 4000-400 cm^{-1}. Single crystal X-ray diffraction data were collected on a Bruker APEX II diffractometer using Mo-Kα monochromatized radiation (λ = 0.71073Å) at 296 K. TG analysis was performed on a Diamond TG-DSC thermal analyzer in flowing N_2 with a heating rate of 10 °C min^{-1}. X-ray powder diffraction data were obtained on Bruker D8X diffractometer using Cu-Kα monochromatized radiation (λ = 1.5418 Å) in the 2θ range of 5-50° at room temperature.

2. Esterification of phosphoric acid with equimolar lauryl alcohol

The esterification of lauryl alcohol with equimolar phosphoric acid was performed in a 100ml three-necked round-bottomed flask. A powder of catalyst, phosphoric acid (0.10 mol, 85%

aqueous solution), and lauryl alcohol (0.10 mol) were charged into the flask.

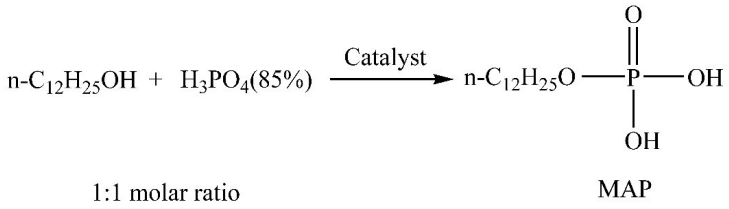

Scheme S1. Esterification of phosphoric acid with equimolar lauryl alcohol into MAP.

3. Synthesis

Synthesis of compound 1

A mixture of $Co(OAc)_2 \cdot 4H_2O$ (0.125 g, 0.50 mmol), DAPSC (0.020 g, 0.07 mmol), $K_5BW_{12}O_{40} \cdot 11.4H_2O$ (0.100 g, 0.03 mmol), and 10 ml H_2O was stirred at room temperature for 30 min. Then the resulting solution was sealed in a 20 ml Teflon-line autoclave and kept at 80 °C for 3 days. After slowly cooling to room temperature, yellow schistose crystals (Fig. S1) of **1** were filtered, washed with distilled water, and dried in a desiccator to give a yield of 67 % (0.0723 g) based on DAPSC. Elemental analysis: Calcd (%): C, 8.56; H, 1.45; N, 6.35. Found (%): C, 8.49; H, 1.37; N, 6.30. IR of compound **1** (cm^{-1}): 3416 (b), 2924 (s), 2854 (m), 1665 (s), 1384 (s), 999 (m), 953 (m), 914 (m), 826 (s).

Synthesis of compound 2

Compound **2** was prepared similarly to compound **1**, except that 0.50 mmol $Zn(OAc)_2 \cdot 2H_2O$ was used instead of $Co(OAc)_2 \cdot 4H_2O$. Light yellow needle crystals (Fig. S2) of **2** were filtered, washed with distilled water, and dried in a desiccator to give a yield of 69 % (0.0747 g) based on DAPSC. Elemental analysis: Calcd (%): C, 8.56; H, 1.40; N, 6.35. Found (%): C, 8.42; H, 1.35; N, 6.28. IR of compound **2** (cm^{-1}): 3416 (b), 2924 (s), 2851 (m), 1665 (s), 1384 (s), 998 (m), 953 (m), 913 (m), 827 (s).

4. Supplementary crystal Selected bond distances, bond angles and Structural Figures.

Single crystal X-ray diffraction data of compounds **1** and **2** were collected on a Bruker APEX II diffractometer using Mo-Kα monochromatized radiation (λ = 0.71073 Å) at 296 K. Empirical absorption correction was applied. Crystal structures were solved by direct method and refined by

full-matrix least-squares method on F^2 using the SHELXTL-2014 software package. Anisotropic thermal parameters were used to refine all non-hydrogen atoms. Since both structures include lots of heavy W atoms, the H atoms of water are not located. Also the thermal parameters of some C, N, and O atoms are restrained. A summary of the crystallographic data and structure determination for two compounds are provided in Table S1. Selected bond lengths and angles for compounds **1** and **2** are given in Table S2-S3.

Table. S1 The Crystallographic data of compounds **1** and **2.**

Compound	**1**	**2**
Empirical formula	$C_{55}H_{111}N_{35}O_{108}B_2Co_5W_{24}$	$C_{55}H_{107}N_{35}O_{106}B_2Zn_5W_{24}$
Formula weight	7719.45	7715.62
Temperature (K)	296(2)	296(2)
Wavelength (Å)	0.71073	0.71073
Crystal system	Triclinic	Triclinic
Space group	P-1	P-1
a (Å)	13.2288(16)	13.0563(13)
b (Å)	23.019(3)	22.736(2)
c (Å)	25.386(3)	25.199(3)
α (°)	87.375(2)	87.6450(10)
β (°)	80.115(2)	79.8300(10)
γ (°)	85.161(2)	84.8880(10)
Volume ($Å^3$)	7584.7(16)	7331.1(13)
Z	2	2
Calculated density (Mg / m^3)	3.380	3.495
Absorption coefficient (mm^{-1})	18.758	19.657
F(000)	6942	6932
Crystal size (mm^3)	0.12 × 0.06 × 0.02	0.12 × 0.02 × 0.02
Limiting indices	-16<=h<=15 -27<=k<=27 -30<=l<=30	-14<=h<=15 -25<=k<=27 -30<=l<=30
Reflections collected	55248	52966
Independent reflection	27484 [R(int) = 0.0570]	26535 [R(int) = 0.0619]
Completeness (%)	98.4	98.1
Refinement method	Full-matrix least-squares on F^2	Full-matrix least-squares on F^2
Data / restraints / parameters	27484 / 311 / 2072	26535 / 1180 / 2053
Goodness-of-fit on F^2	1.024	1.066
Final R indices [I > 2sigma(I)]	R_1 = 0.0524, wR_2 = 0.1300	R_1 = 0.0711, wR_2 = 0.1506
R indices (all data)	R_1 = 0.0877, wR_2 = 0.1459	R_1 = 0.1223, wR_2 = 0.1682

[a] $R_1 = \Sigma||F_o|-|F_c||/\Sigma|F_o|$; $wR_2 = \Sigma[w(F_o^2-F_c^2)^2]/\Sigma[w(F_o^2)^2]^{1/2}$

Table. S2 Selected bond lengths and angles for **1**

Co(1)-O(1W)	2.135(8)	Co(3)-O(85)	2.182(9)
Co(1)-O(2W)	2.158(7)	Co(3)-O(84)	2.206(9)
Co(1)-O(59)	2.180(8)	Co(3)-N(19)	2.207(9)
Co(1)-O(42)	2.190(7)	Co(4)-O(6W)	2.128(9)
Co(1)-N(3)	2.195(10)	Co(4)-O(10)	2.137(8)
Co(1)-N(4)	2.196(9)	Co(4)-N(24)	2.188(10)
Co(1)-N(5)	2.224(10)	Co(4)-O(63)	2.195(9)
Co(2)-N(11)	2.151(8)	Co(4)-N(25)	2.199(9)
Co(2)-O(1)	2.152(8)	Co(4)-N(26)	2.207(11)
Co(2)-O(82)	2.160(8)	Co(4)-O(77)	2.208(8)
Co(2)-N(10)	2.186(10)	Co(5)-O(8W)	2.123(11)
Co(2)-N(12)	2.198(9)	Co(5)-N(32)	2.137(13)
Co(2)-O(30)	2.229(8)	Co(5)-O(89)	2.139(10)
Co(2)-O(3W)	2.234(8)	Co(5)-N(33)	2.142(12)
Co(3)-N(18)	2.114(11)	Co(5)-O(7W)	2.172(11)
Co(3)-O(5W)	2.147(9)	Co(5)-N(31)	2.178(12)
Co(3)-O(4W)	2.154(10)	Co(5)-O(90)	2.221(11)
Co(3)-N(17)	2.181(10)	N(31)-Co(5)-O(90)	148.3(4)
O(1W)-Co(1)-O(2W)	172.5(3)	N(17)-Co(3)-O(85)	71.9(3)
O(1W)-Co(1)-O(59)	85.6(2)	N(18)-Co(3)-O(84)	140.6(3)
O(2W)-Co(1)-O(59)	90.6(2)	O(5W)-Co(3)-O(84)	94.4(2)
O(1W)-Co(1)-O(42)	87.4(2)	O(4W)-Co(3)-O(84)	86.0(3)
O(2W)-Co(1)-O(42)	85.4(2)	N(17)-Co(3)-O(84)	148.3(3)
O(59)-Co(1)-O(42)	76.8(3)	O(85)-Co(3)-O(84)	76.6(3)
O(1W)-Co(1)-N(3)	92.3(3)	N(18)-Co(3)-N(19)	71.1(4)
O(2W)-Co(1)-N(3)	92.6(3)	O(5W)-Co(3)-N(19)	87.5(3)
O(59)-Co(1)-N(3)	70.9(2)	O(4W)-Co(3)-N(19)	98.2(4)
O(42)-Co(1)-N(3)	147.6(2)	N(17)-Co(3)-N(19)	142.2(4)
O(1W)-Co(1)-N(4)	94.6(3)	O(85)-Co(3)-N(19)	145.7(3)
O(2W)-Co(1)-N(4)	92.4(3)	O(84)-Co(3)-N(19)	69.5(3)
O(59)-Co(1)-N(4)	141.6(3)	O(6W)-Co(4)-O(10)	169.2(3)
O(42)-Co(1)-N(4)	141.7(3)	O(6W)-Co(4)-N(24)	83.0(4)
N(3)-Co(1)-N(4)	70.6(4)	O(10)-Co(4)-N(24)	92.3(3)
O(1W)-Co(1)-N(5)	92.7(3)	O(6W)-Co(4)-O(63)	84.7(3)
O(2W)-Co(1)-N(5)	87.1(3)	O(10)-Co(4)-O(63)	84.6(3)
O(59)-Co(1)-N(5)	148.4(2)	N(24)-Co(4)-O(63)	72.9(3)
O(42)-Co(1)-N(5)	71.6(2)	O(6W)-Co(4)-N(25)	94.8(4)
N(3)-Co(1)-N(5)	140.6(3)	O(10)-Co(4)-N(25)	92.5(2)
N(4)-Co(1)-N(5)	70.0(4)	N(24)-Co(4)-N(25)	68.9(4)
N(11)-Co(2)-O(1)	92.2(2)	O(63)-Co(4)-N(25)	141.5(2)
N(11)-Co(2)-O(82)	142.1(3)	O(6W)-Co(4)-N(26)	97.6(4)
O(1)-Co(2)-O(82)	87.2(3)	O(10)-Co(4)-N(26)	92.2(2)
N(11)-Co(2)-N(10)	71.0(3)	N(24)-Co(4)-N(26)	140.0(4)

O(1)-Co(2)-N(10)	84.8(2)	O(63)-Co(4)-N(26)	147.1(2)
O(82)-Co(2)-N(10)	146.3(2)	N(25)-Co(4)-N(26)	71.3(3)
N(11)-Co(2)-N(12)	70.3(3)	O(6W)-Co(4)-O(77)	89.1(3)
O(1)-Co(2)-N(12)	92.0(2)	O(10)-Co(4)-O(77)	90.1(3)
O(82)-Co(2)-N(12)	71.9(2)	N(24)-Co(4)-O(77)	149.8(3)
N(10)-Co(2)-N(12)	140.9(3)	O(63)-Co(4)-O(77)	77.4(3)
N(11)-Co(2)-O(30)	142.1(3)	N(25)-Co(4)-O(77)	141.0(2)
O(1)-Co(2)-O(30)	89.2(3)	N(26)-Co(4)-O(77)	69.8(2)
O(82)-Co(2)-O(30)	75.8(3)	O(8W)-Co(5)-N(32)	92.3(5)
N(10)-Co(2)-O(30)	71.5(2)	O(8W)-Co(5)-O(89)	90.8(4)
N(12)-Co(2)-O(30)	147.5(2)	N(32)-Co(5)-O(89)	142.6(4)
N(11)-Co(2)-O(3W)	90.2(3)	O(8W)-Co(5)-N(33)	92.8(5)
O(1)-Co(2)-O(3W)	176.9(2)	N(32)-Co(5)-N(33)	69.2(5)
O(82)-Co(2)-O(3W)	89.8(2)	O(89)-Co(5)-N(33)	147.9(5)
N(10)-Co(2)-O(3W)	97.8(3)	O(8W)-Co(5)-O(7W)	176.9(4)
N(12)-Co(2)-O(3W)	87.1(3)	N(32)-Co(5)-O(7W)	90.8(5)
O(30)-Co(2)-O(3W)	90.0(2)	O(89)-Co(5)-O(7W)	86.9(4)
N(18)-Co(3)-O(5W)	85.0(4)	N(33)-Co(5)-O(7W)	88.1(5)
N(18)-Co(3)-O(4W)	98.5(4)	O(8W)-Co(5)-N(31)	86.0(5)
O(5W)-Co(3)-O(4W)	174.0(3)	N(32)-Co(5)-N(31)	70.3(5)
N(18)-Co(3)-N(17)	71.1(4)	O(89)-Co(5)-N(31)	72.8(4)
O(5W)-Co(3)-N(17)	88.4(4)	N(33)-Co(5)-N(31)	139.3(5)
O(4W)-Co(3)-N(17)	88.1(4)	O(7W)-Co(5)-N(31)	95.3(5)
N(18)-Co(3)-O(85)	142.7(3)	O(8W)-Co(5)-O(90)	87.8(4)
O(5W)-Co(3)-O(85)	90.2(2)	N(32)-Co(5)-O(90)	141.0(4)
O(4W)-Co(3)-O(85)	84.1(3)	O(89)-Co(5)-O(90)	76.3(4)
O(7W)-Co(5)-O(90)	89.7(4)	N(33)-Co(5)-O(90)	71.9(5)

Table. S3 Selected bond lengths and angles for **2**

Zn(1)-O(1W)	2.102(11)	Zn(3)-O(85)	2.247(13)
Zn(1)-O(2W)	2.123(10)	Zn(3)-N(19)	2.251(14)
Zn(1)-O(42)	2.177(10)	Zn(3)-O(84)	2.284(12)
Zn(1)-N(4)	2.186(12)	Zn(4)-O(10)	2.094(12)
Zn(1)-O(59)	2.207(11)	Zn(4)-O(6W)	2.11(2)
Zn(1)-N(3)	2.218(14)	Zn(4)-N(26)	2.186(18)
Zn(1)-N(5)	2.243(13)	Zn(4)-O(77)	2.195(12)
Zn(2)-O(1)	2.132(10)	Zn(4)-N(24)	2.21(2)
Zn(2)-O(82)	2.172(11)	Zn(4)-O(63)	2.263(19)
Zn(2)-O(3W)	2.189(11)	Zn(4)-N(25)	2.27(2)
Zn(2)-N(11)	2.195(13)	Zn(5)-O(8W)	2.092(15)
Zn(2)-N(10)	2.203(12)	Zn(5)-O(7W)	2.122(16)
Zn(2)-N(12)	2.205(13)	Zn(5)-O(89)	2.184(17)
Zn(2)-O(30)	2.228(10)	Zn(5)-N(32)	2.199(15)
Zn(3)-O(4W)	2.091(12)	Zn(5)-N(31)	2.209(19)

Zn(3)-O(5W)	2.091(11)	Zn(5)-N(33)	2.239(17)
Zn(3)-N(18)	2.131(15)	Zn(5)-O(90)	2.302(17)
Zn(3)-N(17)	2.194(14)	N(33)-Zn(5)-O(90)	69.1(6)
O(1W)-Zn(1)-O(2W)	170.2(4)	O(4W)-Zn(3)-N(19)	100.9(5)
O(1W)-Zn(1)-O(42)	87.0(3)	O(5W)-Zn(3)-N(19)	87.3(5)
O(2W)-Zn(1)-O(42)	83.6(3)	N(18)-Zn(3)-N(19)	70.7(5)
O(1W)-Zn(1)-N(4)	95.1(4)	N(17)-Zn(3)-N(19)	142.3(5)
O(2W)-Zn(1)-N(4)	94.0(4)	O(85)-Zn(3)-N(19)	146.2(4)
O(42)-Zn(1)-N(4)	140.9(3)	O(4W)-Zn(3)-O(84)	82.8(3)
O(1W)-Zn(1)-O(59)	85.4(3)	O(5W)-Zn(3)-O(84)	92.8(3)
O(2W)-Zn(1)-O(59)	89.8(3)	N(18)-Zn(3)-O(84)	139.4(4)
O(42)-Zn(1)-O(59)	77.9(4)	N(17)-Zn(3)-O(84)	148.9(4)
N(4)-Zn(1)-O(59)	141.2(3)	O(85)-Zn(3)-O(84)	78.0(4)
O(1W)-Zn(1)-N(3)	91.2(5)	N(19)-Zn(3)-O(84)	68.8(4)
O(2W)-Zn(1)-N(3)	95.3(4)	O(10)-Zn(4)-O(6W)	157.8(6)
O(42)-Zn(1)-N(3)	148.7(3)	O(10)-Zn(4)-N(26)	95.0(5)
N(4)-Zn(1)-N(3)	70.3(5)	O(6W)-Zn(4)-N(26)	107.1(8)
O(59)-Zn(1)-N(3)	70.8(3)	O(10)-Zn(4)-O(77)	92.6(4)
O(1W)-Zn(1)-N(5)	92.2(4)	O(6W)-Zn(4)-O(77)	92.2(5)
O(2W)-Zn(1)-N(5)	87.5(4)	N(26)-Zn(4)-O(77)	70.5(4)
O(42)-Zn(1)-N(5)	71.3(3)	O(10)-Zn(4)-N(24)	89.5(7)
N(4)-Zn(1)-N(5)	69.7(5)	O(6W)-Zn(4)-N(24)	75.5(9)
O(59)-Zn(1)-N(5)	149.2(3)	N(26)-Zn(4)-N(24)	140.0(8)
N(3)-Zn(1)-N(5)	140.0(5)	O(77)-Zn(4)-N(24)	149.2(7)
O(1)-Zn(2)-O(82)	87.9(4)	O(10)-Zn(4)-O(63)	85.6(6)
O(1)-Zn(2)-O(3W)	177.8(3)	O(6W)-Zn(4)-O(63)	73.8(6)
O(82)-Zn(2)-O(3W)	90.0(3)	N(26)-Zn(4)-O(63)	151.4(5)
O(1)-Zn(2)-N(11)	90.3(3)	O(77)-Zn(4)-O(63)	80.9(6)
O(82)-Zn(2)-N(11)	142.3(3)	N(24)-Zn(4)-O(63)	68.6(7)
O(3W)-Zn(2)-N(11)	91.6(4)	O(10)-Zn(4)-N(25)	92.5(5)
O(1)-Zn(2)-N(10)	80.9(3)	O(6W)-Zn(4)-N(25)	97.3(8)
O(82)-Zn(2)-N(10)	146.0(3)	N(26)-Zn(4)-N(25)	70.6(7)
O(3W)-Zn(2)-N(10)	100.7(4)	O(77)-Zn(4)-N(25)	141.0(5)
N(11)-Zn(2)-N(10)	70.2(5)	N(24)-Zn(4)-N(25)	69.5(9)
O(1)-Zn(2)-N(12)	93.2(3)	O(63)-Zn(4)-N(25)	138.0(5)
O(82)-Zn(2)-N(12)	71.7(3)	O(8W)-Zn(5)-O(7W)	169.8(6)
O(3W)-Zn(2)-N(12)	86.5(4)	O(8W)-Zn(5)-O(89)	87.0(7)
N(11)-Zn(2)-N(12)	70.8(5)	O(7W)-Zn(5)-O(89)	85.6(6)
N(10)-Zn(2)-N(12)	140.5(5)	O(8W)-Zn(5)-N(32)	96.4(6)
O(1)-Zn(2)-O(30)	88.7(4)	O(7W)-Zn(5)-N(32)	93.7(6)
O(82)-Zn(2)-O(30)	76.3(4)	O(89)-Zn(5)-N(32)	143.2(6)
O(3W)-Zn(2)-O(30)	90.4(3)	O(8W)-Zn(5)-N(31)	89.9(7)
N(11)-Zn(2)-O(30)	141.3(3)	O(7W)-Zn(5)-N(31)	94.6(6)
N(10)-Zn(2)-O(30)	71.5(3)	O(89)-Zn(5)-N(31)	72.4(7)

N(12)-Zn(2)-O(30)	147.8(3)	N(32)-Zn(5)-N(31)	70.9(6)
O(4W)-Zn(3)-O(5W)	168.4(5)	O(8W)-Zn(5)-N(33)	90.2(6)
O(4W)-Zn(3)-N(18)	102.6(5)	O(7W)-Zn(5)-N(33)	92.1(6)
O(5W)-Zn(3)-N(18)	87.7(5)	O(89)-Zn(5)-N(33)	147.5(6)
O(4W)-Zn(3)-N(17)	89.3(5)	N(32)-Zn(5)-N(33)	69.3(6)
O(5W)-Zn(3)-N(17)	88.9(5)	N(31)-Zn(5)-N(33)	140.0(6)
N(18)-Zn(3)-N(17)	71.6(5)	O(8W)-Zn(5)-O(90)	84.2(6)
O(4W)-Zn(3)-O(85)	80.3(3)	O(7W)-Zn(5)-O(90)	87.4(6)
O(5W)-Zn(3)-O(85)	88.4(3)	O(89)-Zn(5)-O(90)	78.4(6)
N(18)-Zn(3)-O(85)	142.5(4)	N(32)-Zn(5)-O(90)	138.4(6)
N(17)-Zn(3)-O(85)	71.1(4)	N(31)-Zn(5)-O(90)	150.5(6)

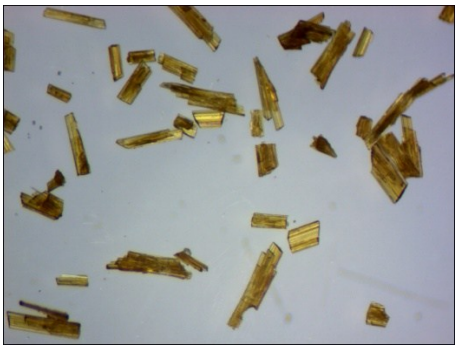

Fig. S1 Microscope image of compound **1**

Fig. S2 Microscope image of compound **2**

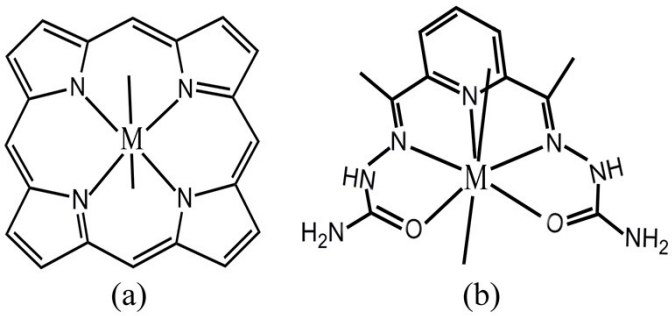

Fig. S3 The coordination models in porphyrin complex (a) and DAPSC (b).

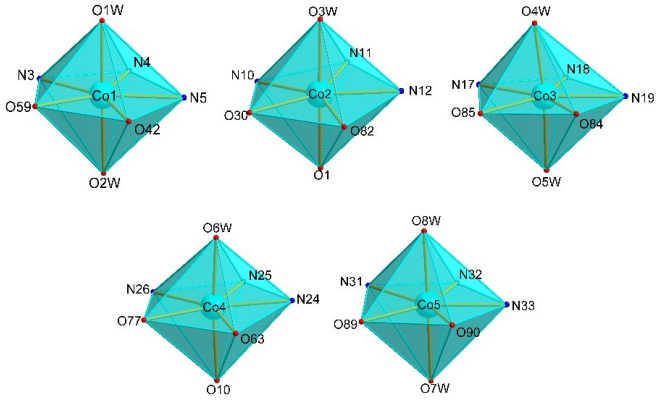

Fig. S4 The coordination modes of Co ion in compound **1**.

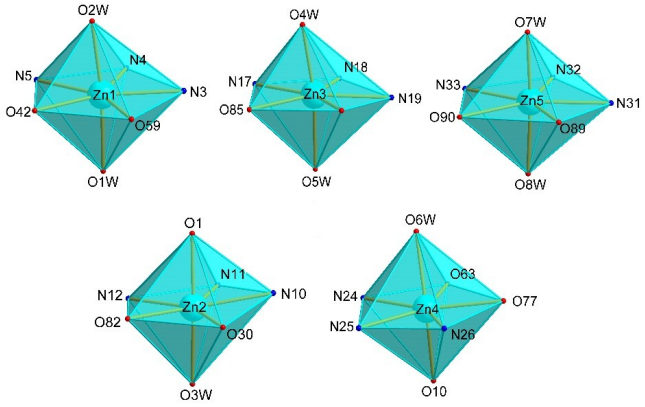

Fig. S5 The coordination modes of Zn ion in compound **2**.

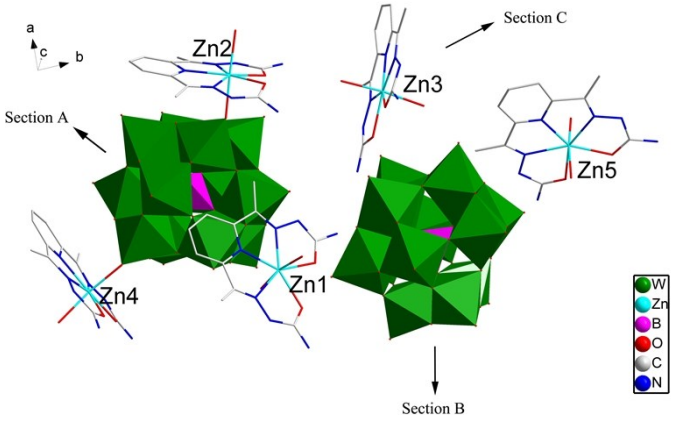

Fig. S6 Stick and polyhedral representation of the asymmetric unit of compound **2**. The hydrogen atoms, crystallization water molecules are omitted for clarity.

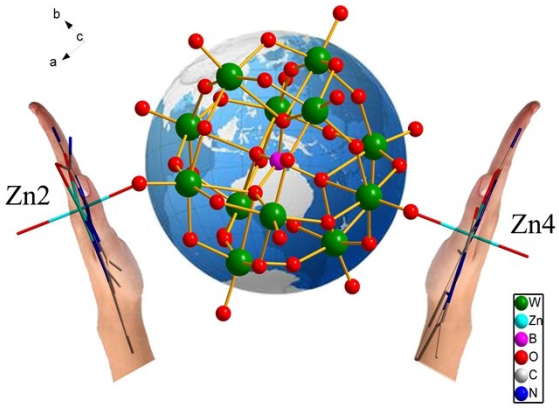

Fig. S7 Ball and Stick representation of Section A in compound **2**.

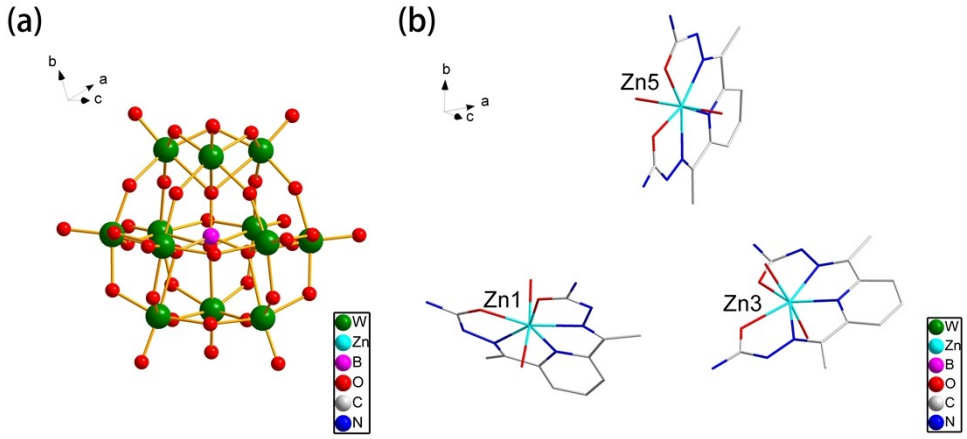

Fig. S8 Ball and Stick representation of Section B (a) and Section C (b) in compound **2**.

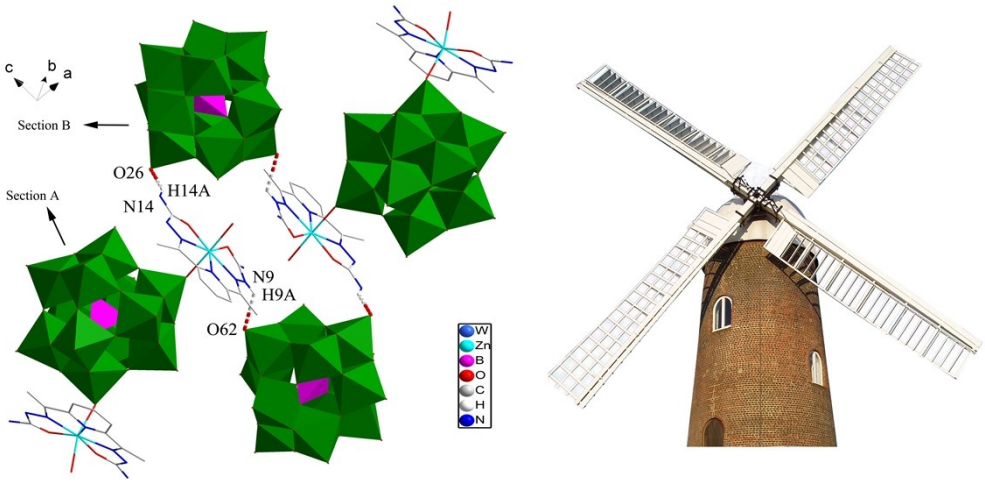

Fig. S9 Stick and polyhedral representation of the symmetrical windmill structure connected via hydrogen bonds in compound **2**.

5. Supplementary Physical Characterizations.

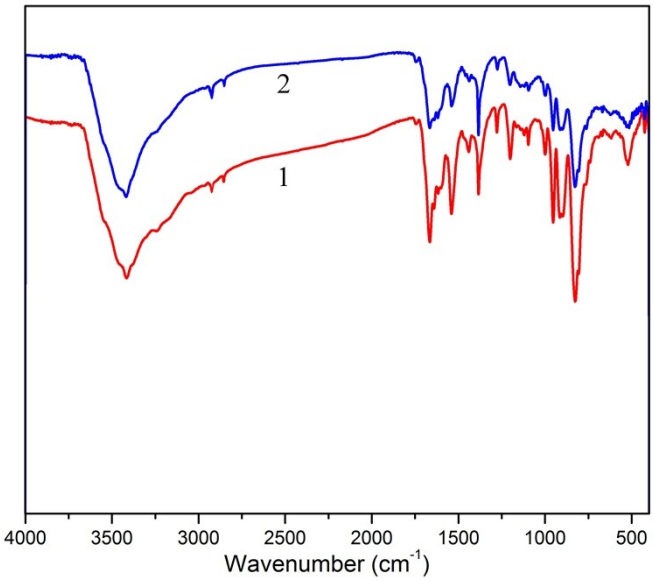

Fig. S10 The IR spectra of compounds **1** (black) and **2** (red)

The IR spectra of compounds **1** and **2** are similar (Fig. S10). For compound **1**, the peak at 999 cm^{-1} could be attributed to υ(B-O), and bands at 826 cm^{-1}, 914 cm^{-1}, 953 cm^{-1} could be associated with υ(W-O-W) and υ(W=O). A series of bands in the region of 1384, 1665, 2854, 2924 cm^{-1} could be ascribed to the character peaks of DAPSC ligand. Additionally, the broad peak at about 3416 cm^{-1} reveals the presence of water molecules in the structure of **1**, which is consistent with the results of single crystal X-ray diffraction analysis. In the spectrum of **2**, the bands at 998, 827, 913, 953 cm^{-1} could be ascribed to υ(B-O), υ(W-O-W) and υ(W=O). A series of bands in the 1384, 1665, 2851, 2924 cm^{-1} could be ascribed to the character peaks of DAPSC ligand. Like **1**, the IR spectrum of **2** also exists a broad band at about 3416 cm^{-1} associated with the water of crystallization. Both compounds **1** and **2** exhibit characteristic peaks of the $[BW_{12}O_{40}]^{5-}$ polyoxoanion. It is noteworthy that compound **2** almost gives the same IR spectrum as compound **1**, which strongly suggests that they have the same molecular structure. Small shifts in the wavelengths of $[BW_{12}O_{40}]^{5-}$ polyoxoanion characteristic peaks may be due to the diverse coordination environment.

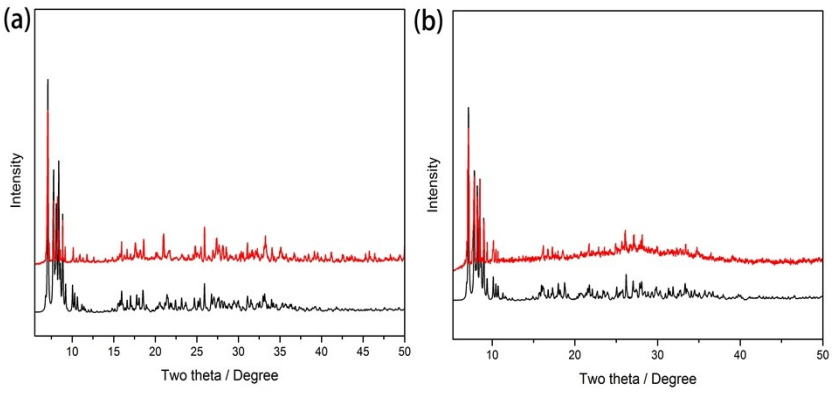

Fig. S11 The simulated (black) and experimental (red) powder X-ray diffraction patterns for **1** (a) and **2** (b).

Powder X-ray diffraction (PXRD) measurements for compounds **1** and **2** were determined at room temperature (Fig. S11). The experimental powder X-ray diffraction patterns of compounds **1** and **2** are consistent with the simulated patterns derived from the single crystal X-ray diffraction data, showing the good purities of the sample phase.

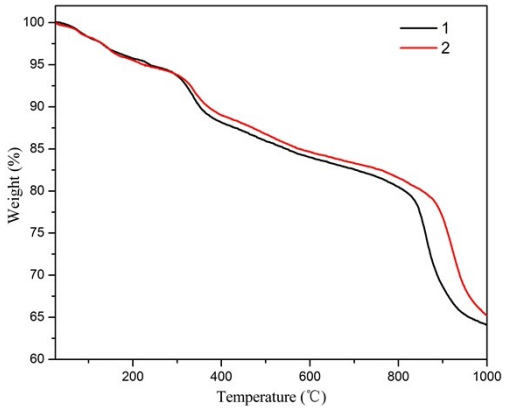

Fig. S12. The TG curves for **1** and **2**.

The thermal gravimetric analyses (TGA) of **1** and **2** are present in the Fig. S12. For compound **1**, TGA show three main steps of weight loss. The first weight loss of 5.18 % (calc. 4.20 %) in the temperature range of 25-250 °C is corresponding to the release of lattice water and coordinated water molecules. As the temperature reaches 250 °C, DAPSC ligands are removed and the framework collapses. Compound 1 lose a mass of 20.66 % (calc. 22.16 %) in the temperature range of 250-800 °C. The final product is the metal oxide. Similar to compound **1**, the TGA of compound **2** also show three main steps of weight loss. The first weight loss of 5.34 % (calc. 3.73 %) in the temperature range of 25-250 °C is associated with the release of lattice water and

coordinated water molecules. The second weight loss of 20.21 % (calc. 21.70 %) at 250-860 °C is ascribed to decomposition of the DAPSC ligands. The final product is the metal oxide.

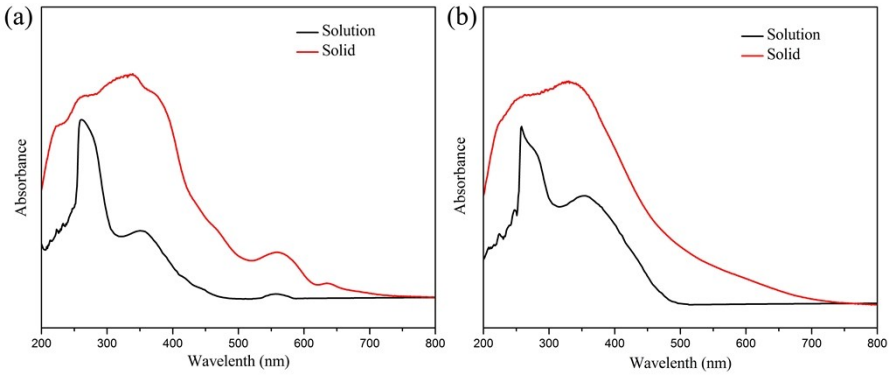

Fig. S13 The UV-Vis absorption spectra of **1** (a) and **2** (b) in the solid and DMSO solution (2×10^{-6} mol·L^{-1}).

As shown in Fig. S13, the UV-Vis absorption spectra of **1** and **2** were recorded in the solid state and DMSO solution (2×10^{-6} mol·L^{-1}). In the spectrum of **1**, there are three main absorption bands. The absorption bond at 260 nm are assigned to O→W charge-transfer transitions in the POMs structure. The second bond at 350 nm corresponds to the π-π* transition within the C=N group. And the last bond is observed at 554 nm due to d-d electron transition of Co center. Similar to **1**, **2** exhibits two main absorption bands around 258 and 351 nm, which are associated with O→W charge-transfer transitions, and the latter one is attributed to the π-π* transition C=N group.

Table S4. Comparison of the catalytic performances of the mixtures of Co-DAPSC complex and POMs at different ratios.[a]

Entry	Catalyst n_A:n_B	Conversion (%)	Selectivity (%) MAP / MDP	
1	1:1	31.92	98.67	1.33
2	2:3	31.52	97.22	2.78
3	1:2	31.21	98.63	1.37
4	2:5	31.78	97.30	2.70
5	1:3	30.98	98.65	1.35

[a] Reaction conditions: {Catalyst A: $K_5BW_{12}O_{40}$ (0.026mmol compared with 0.1 g compounds **1** or **2**), B: [Co(DAPSC)Cl]Cl·$2H_2O$}, lauryl alcohol (0.10 mol), phosphoric acid (0.10 mol), no solvent, 90 °C, 1 h.

Table S5. Comparison of the catalytic performances of the mixtures of Zn-DAPSC complex and POMs at different ratios.[a]

Entry	Catalyst n_A:n_B	Conversion (%)	Selectivity (%) MAP / MDP	
1	1:1	32.01	97.30	2.70
2	2:3	30.95	97.22	2.78
3	1:2	31.85	98.67	1.33
4	2:5	31.60	97.35	2.65
5	1:3	30.43	98.57	1.43

[a] Reaction conditions: Catalyst (A: $K_5BW_{12}O_{40}$, B: $[Zn(DAPSC)Cl]Cl{\cdot}2H_2O$), lauryl alcohol (0.10 mol), phosphoric acid (0.10 mol), no solvent, 90 °C, 1 h.

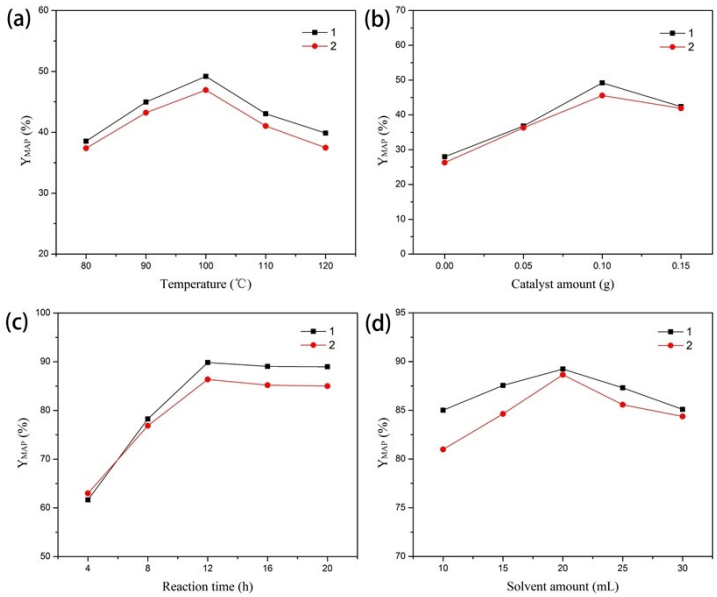

Fig. S14 The yields of MAP at various reaction temperature (a), catalyst amount (b), reaction time (c) and solvent amount (d). Reaction conditions: (a) catalyst (0.10 g), lauryl alcohol (0.10 mol), phosphoric acid (0.10 mol), no solvent, 1 h; (b) lauryl alcohol (0.10 mol), phosphoric acid (0.10 mol), no solvent, 100 °C, 1 h; (c) catalyst (0.10 g), lauryl alcohol (0.10 mol), phosphoric acid (0.10 mol), no solvent, 100 °C; (d) catalyst (0.10 g), lauryl alcohol (0.10 mol), phosphoric acid (0.10 mol), 110 °C, 12 h.

Table. S6 The yield and selectivity of MAP at various reaction temperature. [a]

Catalyst	Temperature (°C)	Yield (%)	Selectivity (%)
1	80	38.54	100
	90	44.97	98.80
	100	49.19	98.85

	110	43.04	97.65
	120	39.87	97.59
2	80	37.38	97.37
	90	42.22	98.77
	100	46.92	97.65
	110	41.02	97.67
	120	37.46	97.56

[a] Reaction conditions: catalyst (0.10 g), lauryl alcohol (0.10 mol), phosphoric acid (0.10 mol), no solvent, 1 h

Table. S7 The yield and selectivity of MAP at various catalyst amount. [b]

Catalyst	Catalyst amount (g)	Yield (%)	Selectivity (%)
1	0.05	36.81	97.53
	0.10	49.19	98.85
	0.15	42.39	97.62
2	0.05	36.29	97.47
	0.10	45.57	97.65
	0.15	41.89	97.59

[b] Reaction conditions: lauryl alcohol (0.10 mol), phosphoric acid (0.10 mol), no solvent, 100 °C, 1 h

Table. S8 The yield and selectivity of MAP at various reaction time. [c]

Catalyst	Reaction Time (h)	Yield (%)	Selectivity (%)
1	4	61.63	98.36
	8	78.26	97.44
	12	89.83	98.88
	16	89.05	97.70
	20	88.95	99.44
2	4	62.98	96.12
	8	76.86	97.47
	12	86.37	98.31
	16	85.18	98.83
	20	85.01	98.87

[c] Reaction conditions: catalyst (0.10 g), lauryl alcohol (0.10 mol), phosphoric acid (0.10 mol), no solvent, 100 °C

Table. S9 The yield and selectivity of MAP at various solvent amount. [d]

Catalyst	Solvent amount (mL)	Yield (%)	Selectivity (%)
	10	85.01	98.86
	15	87.56	100

1	20	89.24	98.88
	25	87.31	99.43
	30	85.09	99.44
2	10	80.99	99.43
	15	84.63	98.84
	20	88.65	98.86
	25	85.57	99.43
	30	84.37	99.43

[d] Reaction conditions: catalyst (0.10 g), lauryl alcohol (0.10 mol), phosphoric acid (0.10 mol), 110 °C, 12 h.

Table. S10 Comparison of the catalytic performances of the various catalysts for the esterification of lauryl alcohol with phosphoric acid.

Entry	Catalyst	Conversion (%)	Selectivity (%) MAP / MDP	
1	No catalyst	52.96	98.06	1.94
2	$K_5BW_{12}O_{40}$	70.86	98.62	1.38
3	DAPSC	35.17	97.18	2.82
4	$Co(Ac)_2{\cdot}4H_2O$	51.52	98.10	1.90
5	$Zn(Ac)_2{\cdot}2H_2O$	52.65	98.08	1.92
6	**1**	90.86	98.88	1.12
7	**2**	87.85	98.31	1.69

Reaction conditions: catalyst (0.10 g), lauryl alcohol (0.10 mol), phosphoric acid (0.10 mol), no solvent, 100 °C, 12 h.